

Molecular enhancement factors for P, T-violating eEDM in BaCH₃ and YbCH₃ symmetric top molecules

Yuly Chamorro, Anastasia Borschevsky, and Steven Hoekstra
*Van Swinderen Institute for Particle Physics and Gravity,
University of Groningen, 9747 AG, Groningen, The Netherlands*

Ephraim Eliav
School of Chemistry, Tel Aviv University, 69978 Tel Aviv, Israel

Nicholas R. Hutzler
*Division of Physics, Mathematics, and Astronomy,
California Institute of Technology, Pasadena, California 91125, USA*

Lukáš F. Pašteka
*Department of Physical and Theoretical Chemistry, Faculty of Natural Sciences,
Comenius University, Mlynská dolina, 84215 Bratislava, Slovakia**
(Dated: August 5, 2022)

High-precision tests of fundamental symmetries are looking for the parity- (P), time-reversal- (T) violating electric dipole moment of the electron (eEDM) as proof of physics beyond the Standard Model. Particularly, in polyatomic molecules, the complex vibrational and rotational structure gives the possibility to reach high enhancement of the P, T-odd effects in moderate electric fields. Additionally, it is possible to increase the statistical sensitivity by using laser cooling. In this work, we calculate the P, T-odd electronic structure parameters W_d and W_s for the promising candidates BaCH₃ and YbCH₃ for the interpretation of future experiments. We employ high-accuracy relativistic coupled cluster methods and systematically evaluate the uncertainties of our computational approach. Compared to other Ba- and Yb-containing molecules, BaCH₃ and YbCH₃ exhibit larger W_d and W_s associated to increased covalent character of the M–C bond. The calculated values are $3.22 \pm 0.11 \times 10^{24} \frac{\text{hHz}}{\text{ecm}}$ and $13.80 \pm 0.35 \times 10^{24} \frac{\text{hHz}}{\text{ecm}}$ for W_d , and $8.42 \pm 0.29 \text{ hkHz}$ and $45.35 \pm 1.15 \text{ hkHz}$ for W_s , in BaCH₃ and YbCH₃, respectively. The robust, accurate, and cost-effective computational scheme reported in this work makes our results suitable for extracting the relevant fundamental properties from future measurements and also can be used to explore other polyatomic molecules sensitive to various violations of fundamental symmetries.

I. INTRODUCTION

The Standard Model of particle physics (SM) is known to be the most successful theory in describing the universe at the smallest scale. This model predicts all the known fundamental particles and explains their interactions via three of the four fundamental forces. However, despite its successful descriptions, SM is known to be an incomplete theory. Several well established experimentally observed facts, such as the matter-antimatter asymmetry and the existence of dark matter [1] and dark energy [2] are not described by the SM. In particular, the matter-antimatter asymmetry requires an amount of charge-parity (CP) violation incompatible with the SM [3]. The incompleteness of the SM is both an incentive and an opportunity to look for physics beyond the Standard Model (BSM), also known as new physics.

High-precision tests of fundamental symmetries are a very effective means of probing BSM physics [4]. Specifically, precision experiments in the sub-microhertz level using atoms and molecules are searching for the electric

dipole moment of the electron (eEDM). The eEDM violates both time-reversal symmetry (T) and parity symmetry (P) and, assuming the CPT theorem, the eEDM thus also violates CP symmetry. In the SM, the eEDM is highly suppressed, and the predicted value is far too small to be measured using current experimental techniques. This has been estimated to be in the order of magnitude of $|d_e^{\text{SM}}| < 10^{-40}$ [5]. On the other hand, the BSM theories predict values in the experimental reach [6, 7], and a measurement of a non-zero value would be an incontrovertible proof of new physics [8].

Presence of the eEDM induces an EDM on paramagnetic molecules [9, 10] which is enhanced due to the internal electric fields. It has been previously shown that this enhancement grows with the atomic number as Z^3 [11] making systems containing heavy atoms ideal for measuring the eEDM. Additionally, the experimental signal is also enhanced when using close-lying opposite parity states – more information can be found in the work of Sandars [12, 13]. In atoms, opposite-parity electronic states are split by $\sim 2 \text{ eV}$, while, in molecules, opposite-parity rotational states are split by $\sim 10^{-5} \text{ eV}$, typically. Consequently, some molecular states can offer a dramatically higher enhancement than the enhance-

* lukas.f.pasteka@uniba.sk

ment found in atoms [14, 15]. Motivated by such enhancements, numerous experiments are being developed using molecules containing heavy atoms. The first experiments using diatomic molecules were performed on TlF in Oxford [14, 16–18], and the current most stringent result has been set in ThO by ACME collaboration; $|d_e^{\text{ThO}}| < 1.1 \times 10^{-29} \text{ e}\cdot\text{cm}$ [19]. Other investigated diatomic molecules include YbF [20], HfF⁺ [21], ThO [19], RaF [22, 23], and BaF [24].

Some diatomic molecules, such as PbO [25], ThO [19], and HfF⁺ [21], have almost degenerate opposite parity (excited) eigenstates, called Ω -doublets, which are used to measure the eEDM. These parity doublets have a small splitting which makes it possible to fully mix (or polarize) them in moderate electric fields. Additionally, the use of Ω -doublets give the possibility to cancel many systematic effects. Unfortunately, due to the complex structure of the Ω -doublets states, it is not possible to take advantage of laser cooling to improve the experimental sensitivity. On the other hand, measurements of the eEDM in diatomic molecules in their ground state, such as BaF [24], YbF [20, 26], and RaF [23], cannot make use of the Ω -doublet states.

Polyatomic molecules emerge as good candidates for eEDM experiments [27, 28]. In contrast to diatomic molecules, in polyatomic molecules it is possible to measure the eEDM in the long-lived close-lying opposite parity eigenstates (K -doublets). In addition, previous works [29–34] have discussed the feasibility of laser cooling of metal-containing molecules composed of a single metal atom bound to a single molecular ligand, such as the symmetric top molecules BaCH₃ and YbCH₃. This is also supported by that fact the lighter CaCH₃ and MgCH₃ exhibit quasi-diagonal Frank–Condon factors [31].

The enhancement of the eEDM interaction in atoms and molecules is usually expressed in terms of the electronic structure parameter W_d . The scalar-pseudoscalar (S-PS) interaction between the electrons and the nucleus is also a P,T-violating interaction expressed in terms of the parameter W_s [35] and is similarly enhanced in atoms and molecules. Both parameters are needed to connect the measured energy shift due to P,T-violation to the eEDM value. Since W_d and W_s can not be measured experimentally, it is necessary to use electronic structure methods to calculate them.

In this work, we report the W_d and W_s parameters for the promising eEDM candidates for future experiments, the BaCH₃ and YbCH₃ molecules. Since the enhancement factor depends mainly on the identity of the heavy atom, it is expected that BaCH₃ and YbCH₃ have similar enhancement factors comparable to other isoelectronic molecules relevant for eEDM experiments, such as BaF, BaOH, and YbF, YbOH [36–39], respectively. However, unlike in the diatomic molecules BaF and YbF, the symmetric top molecules BaCH₃ and YbCH₃ have long-lived K -doublets accessible to experimental measurement with an even smaller splitting than in the linear polyatomic BaOH and YbOH molecules, typically $\leq 1 \text{ MHz}$ [27].

The use of these K -doublets to measure the eEDM in BaCH₃ and YbCH₃ makes it possible to access large enhancement of the eEDM using moderate electric fields, reach a high experimental sensitivity, and avoid many systematic effects.

To calculate the W_d and W_s parameters, we employ high accuracy single reference and Fock-space coupled cluster methods and we explore the effect of the different computational factors on the calculated values. The employed methodology allows us to estimate the uncertainty in the calculated values of W_d and W_s . The accurate and robust computational scheme established in this work may be extended to other polyatomic molecules sensitive to parity-violating effects.

II. METHODOLOGY

The eEDM operator, H^{eEDM} , can be written in terms of a one-body operator [40] (here, and throughout the rest of this section, atomic units are used),

$$H^{\text{eEDM}} = 2icd_e \sum_i \gamma_i^5 \gamma_i^0 \mathbf{p}_i^2, \quad (1)$$

where $\gamma^0, \gamma^1, \gamma^2$, and γ^3 represent the Dirac matrices, $\gamma^5 = i\gamma^0\gamma^1\gamma^2\gamma^3$, \mathbf{p}_i is the momentum of the electron i , and c is the speed of light.

The S-PS interaction can be expressed as

$$H^{\text{S-PS}} = i \frac{G_F}{\sqrt{2}} Z_N k_s \sum_i \gamma_i^0 \gamma_i^5 \rho(\mathbf{r}_{iN}), \quad (2)$$

where G_F is the Fermi constant ($2.2225 \times 10^{-14} \text{ a.u.}$), Z_N is the atomic number of the nucleus N , and $\rho(\mathbf{r}_{iN})$ is the nuclear charge distribution. In equations (1) and (2), d_e and k_s parameterize the eEDM and S-PS interaction, respectively.

To calculate the electronic structure constants W_d and W_s using the coupled cluster approach, we use the finite field method [41, 42], similar to our earlier works [37, 38, 43–46].

The total Hamiltonian H is expressed as a sum of a zeroth-order Hamiltonian $H^{(0)}$ and a perturbation H_k , regulated by the field strength parameter λ_k ,

$$H = H^{(0)} + \lambda_k H_k. \quad (3)$$

In our case, $H^{(0)}$ is the unperturbed molecular Dirac-Coulomb Hamiltonian,

$$H^{(0)} = \sum_i [\beta_i mc^2 + c\boldsymbol{\alpha}_i \cdot \mathbf{p}_i - V_{\text{nuc}}(\mathbf{r}_i)], \quad (4)$$

where $\boldsymbol{\alpha}_i$ and β_i are the Dirac matrices and V_{nuc} is the Coulomb potential. Considering the perturbations H^{eEDM} and $H^{\text{S-PS}}$,

$$H_k = \frac{H^{\text{eEDM}}}{d_e}, \quad \frac{H^{\text{S-PS}}}{k_s}, \quad (5)$$

and applying the Hellman–Feynman theorem, the W_d and W_s coupling constants can be calculated as the first derivatives of the energy with respect to λ_k ,

$$W_d = \frac{1}{\Omega} \left\langle \Psi_{\Omega}^{(0)} \left| \frac{H^{e\text{EDM}}}{d_e} \right| \Psi_{\Omega}^{(0)} \right\rangle = \frac{1}{\Omega} \left. \frac{dE_{\Omega}(\lambda_{d_e})}{d\lambda_{d_e}} \right|_{\lambda_{d_e}=0} \quad (6)$$

and

$$W_s = \frac{1}{\Omega} \left\langle \Psi_{\Omega}^{(0)} \left| \frac{H^{\text{S-PS}}}{k_s} \right| \Psi_{\Omega}^{(0)} \right\rangle = \frac{1}{\Omega} \left. \frac{dE_{\Omega}(\lambda_{k_s})}{d\lambda_{k_s}} \right|_{\lambda_{k_s}=0}, \quad (7)$$

where $\Psi_{\Omega}^{(0)}$ is the unperturbed ground state electronic molecular wave function and Ω is the projection of the total electronic angular momentum on the internuclear axis.

The W_d and W_s constants are combined in the P,T-odd effective Hamiltonian, $H^{\text{P,T-odd}}$ [35],

$$H^{\text{P,T-odd}} = (W_d d_e + W_s k_s) \mathbf{S} \cdot \mathbf{n}, \quad (8)$$

where \mathbf{S} is the effective spin and \mathbf{n} is a unit vector oriented along the internuclear axis. Therefore, a measurement of the P,T-violating energy difference on a single molecule provides us with the combined d_e and k_s and the disentanglement of the two effects requires experiments on different molecules [47].

III. RESULTS

In this work we assay a cost-accuracy balanced methodology that allows us to study polyatomic molecules promising for precision experiments, such as BaCH_3 and YbCH_3 , at the high accuracy coupled cluster level. We study the effect of the treatment of relativity and electron correlation and the choice of the basis set on the optimised molecular geometries (section III A) and on the calculated W_d and W_s parameters (section III B). Finally, we estimate the uncertainty of the predicted W_d and W_s based on an extensive computational study within the presented methodology (section III C).

All the calculations were carried out using a modified version of the Dirac 2019 program [48, 49], except for the scalar relativistic (SR) calculations, where the CFOUR program [50, 51] was employed. If not stated otherwise, the default settings of the corresponding codes were used. We applied both the single reference coupled cluster with single, double and perturbative triple excitations (CCSD(T)) [52] and the Fock-space coupled cluster (FSCC) with single and double excitations approach using sector (0,1) [53]. We used the uncontracted Dyall’s relativistic basis sets [54–56] and the contracted atomic natural orbital correlation consistent ANO-RCC basis sets [57–60] of double-, triple-, quadruple-, and quintuple-zeta (for the ANO-RCC basis sets only) cardinality.

A. Geometry optimisation

The spectroscopic properties and the geometries of the polyatomic molecules that are considered to be good candidates for measurements of P,T-violating phenomena are usually not known *a priori*, meaning that any computational study of these systems should begin with a geometry optimisation.

Due to the large number of electrons, geometry optimisation of polyatomic molecules at the 4-component coupled cluster level requires impractically high computational resources. We thus look for a compromise that allows sufficiently accurate calculations at a realistic computational cost. In the Appendix VI A we describe the effects of the relevant computational parameters on the optimised geometry and use these investigations to select the optimal computational approach. After evaluating the effect of treatment of relativity, use of contracted vs. uncontracted basis set, and electron correlation, we conclude that a suitable methodology for reliable geometry optimisations of small polyatomic molecules is the combination of the SR-CCSD/CCSD(T) approach with the contracted ANO-RCC basis sets and correlating the valence and core-valence ($(n-1)$ and $(n-2)$) electrons.

Use of large basis sets is indispensable for taking full advantage of high accuracy correlation methods such as coupled cluster and for getting a good quality description of the system. Table I and Figure 1 show the convergence of the obtained geometry of the two molecules with the increase of the cardinality of the ANO-RCC basis set. The optimised geometry of BaCH_3 (converged at the 5z basis set level) is close (0.3 – 0.7% difference) to the experimental geometry estimated from rotational constants in a gas-phase detection experiment (Ba–C bond distance 2.557 – 2.570 Å, BaCH angle 103° – 108°, both assuming C–H bond distance 1.1 Å) [61]. This slight underestimation is most likely due to the combined effects of scalar relativity and basis set contraction, as can be seen from Table X in Appendix VI A. We evaluate the effect of this discrepancy on the W_d and W_s parameters and include it as a source of uncertainty in our reported values (see Section III C).

In YbCH_3 , we found a faster convergence than in BaCH_3 , and thus used the geometry obtained with the QZ basis set. The optimised geometries used for the calculations of the W_d and W_s parameters in the following sections are presented in bold font in Table I.

B. Enhancement factors: Computational parameters

Both the W_d and W_s factors are purely relativistic properties and, according to Schiff’s theorem, in the non-relativistic regime the atom or the molecule would not have an EDM even if the electron did [62]. However, Schiff’s theorem is not valid in the relativistic regime, and atoms and molecules may express a non-zero EDM

n	Ba-C [Å]	C-H [Å]	BaCH [°]
2	2.61	1.11	113
3	2.58	1.10	113
4	2.56	1.09	113
5	2.55	1.10	113
Expt. [61]	2.557 – 2.570	1.1	103 – 108
n	Yb-C [Å]	C-H [Å]	YbCH [°]
2	2.47	1.11	112
3	2.38	1.09	111
4	2.39	1.09	112

TABLE I. Effect of basis set cardinality (ANO-RCC-VnZP basis sets) on the optimised geometry of BaCH₃ and YbCH₃ at the SR-CCSD(T) level of theory and correlating 37 and 51 electrons, respectively. The final optimised geometries are highlighted in bold.

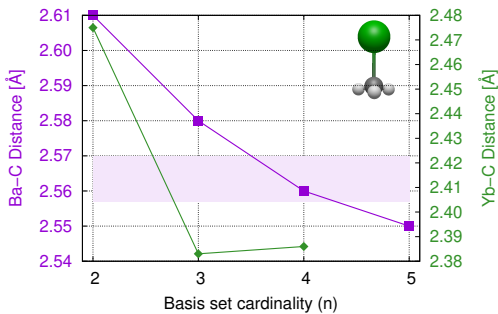


FIG. 1. Convergence of the M -C bond length (M : Ba, Yb) with basis set cardinality (ANO-RCC-VnZP basis sets). The calculations were carried out at the SR-CCSD(T) level of theory and correlating 37 and 51 electrons, respectively. The shaded area corresponds to the experimental bond range distance Ba-C in BaCH₃.

[12]. Therefore, calculations of the W_d and W_s factors should be carried out in a relativistic framework.

In this work, we use the relativistic Dirac-Coulomb 4-component Hamiltonian combined with the single-reference coupled cluster approximation [52] for the calculation of the W_d and W_s factors in BaCH₃, and the multireference Fock-space coupled cluster approach [53], for the corresponding calculations in YbCH₃.

Earlier calculations of the electric-field gradients in YbF [63] and of W_d in YbF [37] and YbOH [38] have shown that Yb-containing molecules may present a multireference character in their ground states. In this work, we found, through the T1 diagnostic [64], that the ground state of YbCH₃ does, indeed, could indeed benefit from Fock space coupled cluster method. In the FSCC(0,1) approach, the starting point is the closed shell ground state of YbCH₃⁺ molecule to which one electron is added within the correlation procedure. In this work, we added the electron to the lowest energy σ orbital, thus using a minimal model space. The consideration of higher energy orbitals through a larger model space was not shown to have a significant effect on the value of W_d in YbF and YbOH [37, 38].

We apply equations (6) and (7) for the calculations of

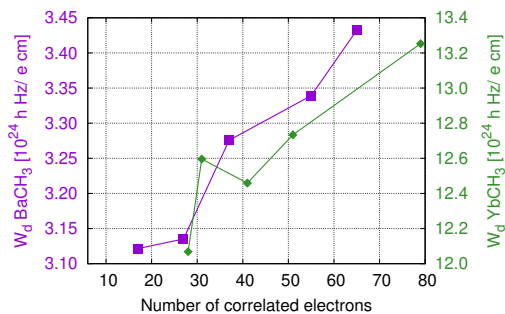


FIG. 2. Effect of the number of correlated electrons, N , on the calculated W_d constants. Values presented in Table II.

both the W_d and W_s factors, using $\lambda_{d_e} = 10^{-8}$ a.u. and $\lambda_{k_s} = 10^{-7}$ a.u. for BaCH₃ and $\lambda_{d_e} = \lambda_{k_s} = 10^{-6}$ a.u. for YbCH₃. These field strengths were selected guaranteeing numerical stability as it is shown in Appendix VI B. In all cases, the convergence criteria of the coupled cluster energy as well as the Hartree-Fock energy was fixed in the $1 \times 10^{-11} - 5 \times 10^{-11}$ a.u. range.

In the following, we present the recommended W_d and W_s values and their uncertainties and discuss the scheme we use to determine the latter, focusing separately on the various parameters that determine the quality of the calculations. Initially, we focus our study on W_d , and subsequently, we include W_s in our discussion.

1. Electron correlation

In this work, we investigate the effect of various computational parameters within the relativistic coupled cluster approach on the calculated W_d and W_s factors.

a. Correlation space Table II and Figure 2 present the CCSD results obtained correlating a different number of electrons; in all these calculations, the virtual cut-off was adjusted symmetrically to the number of electrons correlated (that is the positive energy cut-off was taken to be of the same absolute size as the negative energy cut-off). We observe that correlating only the outer-core-valence electrons (17 electrons in BaCH₃; Ba: 5s; 5p; 6s, C: 2s; 2p, H: 1s, and 29 electrons in YbCH₃; Yb: 5p; 4f; 6s, C: 2s; 2p, H: 1s) causes relative errors of $\sim 9\%$ compared to the value obtained when all the electrons are included in the correlation treatment. Previously, we found that correlating only outer-core-valence electrons in the isoelectronic BaF also led to an error of $\sim 10\%$ compared to the all-electron calculation [37].

Therefore, for the recommended values, all the electrons were correlated. Note that the strong dependence on the description of the core region is unusual for most other atomic and molecular properties, such as molecular geometries or spectra.

Correlation of all the electrons in the coupled cluster approach requires simultaneous inclusion of a proportionally large number of virtual orbitals. Notice that the

N	Frozen orb.		W_d [$10^{24} \frac{\text{hHz}}{\text{e cm}}$]
	Ba	C	
17	[Kr]4d	[He]	3.12 (-9.1%)
27	[Kr]	[He]	3.14 (-8.7%)
37	[Ar]3d	-	3.28 (-4.6%)
55	[Ne]	-	3.34 (-2.7%)
65	-	-	3.43
N	Frozen orb.		W_d [$10^{24} \frac{\text{hHz}}{\text{e cm}}$]
	Yb	C	
29	[Kr]4d5s	[He]	12.07 (-8.9%)
31	[Kr]4d	[He]	12.60 (-5.0%)
41	[Kr]	[He]	12.46 (-6.0%)
51	[Ar]3d	-	12.73 (-3.9%)
79	-	-	13.25

TABLE II. Effect of the number of correlated electrons, N , on the calculated W_d constants. Error relative to the all-electrons-correlated result is presented in parenthesis. Relativistic CCSD and FSCC approaches for BaCH₃ and YbCH₃, respectively, were used, combined with the dyall.v2z basis sets.

Cut-off [a.u.]	W_d [$10^{24} \frac{\text{hHz}}{\text{e cm}}$]	
	BaCH ₃	YbCH ₃
100	3.36 (-2.1%)	13.00 (-1.9%)
500	3.41 (-0.8%)	13.18 (-0.6%)
1000	3.42 (-0.5%)	13.24 (-0.1%)
2000	3.43 (-0.03%)	13.25
3000	3.43	-

TABLE III. Effect of the virtual space cut-off on the calculated W_d constants. Error relative to the highest virtual cut-off value is presented in parenthesis. Relativistic CCSD and FSCC approaches for BaCH₃ and YbCH₃, respectively, were used, combined with the dyall.v2z basis sets. All electrons were correlated.

symmetric virtual cut-off is ~ 1400 a.u. in BaCH₃ and ~ 2300 a.u. in YbCH₃. Figure 3 and Table III present the effect of the virtual cut-off on the calculated W_d , where all the electrons are correlated. According to the results obtained using virtual cut-offs of 1000 and 2000 a.u., increasing the cut-off over 1000 a.u. changes the reported W_d by less than 0.5% for BaCH₃ and by less than 0.1% for YbCH₃. In fact, W_d in BaCH₃ changes by only 0.03% when the virtual cut-off is further increased to 3000 a.u. Therefore, we include all the virtual orbitals until 2000 a.u. in our recommended values, and we use the difference between the results obtained with a virtual cut-off of 2000 and of 1000 a.u. to estimate the uncertainty from neglecting virtual orbitals above 2000 a.u. in the description of the electron correlation. Furthermore, we conclude that when computational resources are a bottleneck, lower cut-off of 500 a.u. can be used, without notable deterioration of the quality of the results.

b. Excitation rank The results discussed so far were obtained at the coupled cluster (either single reference or Fock-space) level of theory with single and double excitations.

We evaluated the effect of triple excitations comparing

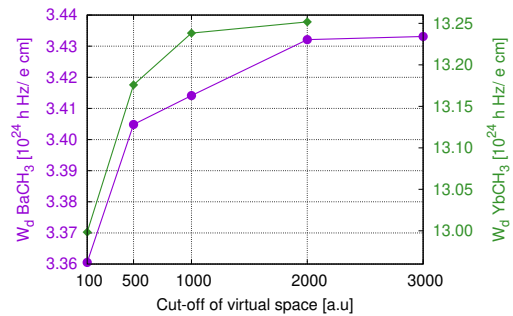


FIG. 3. Effect of the virtual space cut-off on the calculated W_d constants. Values presented in Table III.

Basis set	W_d BaCH ₃ [$10^{24} \frac{\text{hHz}}{\text{e cm}}$]	
	CCSD	CCSD(T)
dyall.v2z	3.12 (+0.6%)	3.10
dyall.v3z	3.01 (+1.0%)	2.98
dyall.v4z	2.95 (+1.3%)	2.91

TABLE IV. Effect of inclusion of triple excitations on the calculated W_d constants. The relative error of CCSD comparing to the perturbative CCSD(T) is presented in parenthesis. 17 electrons were correlated and the virtual cut-off was set to 30 a.u.

the calculated W_d of BaCH₃ at the CCSD and CCSD(T) levels using the 2z, 3z, and 4z quality basis sets (Table IV). In all the cases, the inclusion of triple excitations slightly reduces the calculated W_d . The contribution of the triple excitations increases with the cardinality of the basis set, as expected, but even at the 4z basis set cardinality reaches only 1.3%. The magnitude of this contribution is close to what was observed in previous calculations on BaOH (1.4%) and BaF (1.5%) and suggests that the triple excitations can be neglected when the computational resources are an issue. We report the final W_d and W_s at the CCSD(T) level and use the triples contribution to estimate the uncertainty due to neglecting higher-order excitations.

The use of the FSCC approach allows us to obtain accurate values of W_d and W_s in an open shell system like YbCH₃. However, as perturbative triple excitations are not yet implemented in the FSCC module of the DIRAC program, we can not use this method to perform a reliable calculation of the contribution of the triple and higher-order excitations. Therefore, we do use the difference between the single reference CCSD and CCSD(T) results in BaCH₃ to estimate the relative uncertainty due to the neglect of the triple excitations in YbCH₃ molecule.

2. Basis sets

Next to the electron correlation, the quality of the basis set plays a crucial role in accurate theoretical description of molecular properties. In the following subsections

Basis set	$W_d [10^{24} \frac{\text{hHz}}{\text{ecm}}]$	
	BaCH ₃	YbCH ₃
dyall.v2z	3.10 (+8.3%)	12.07 (-4.4%)
dyall.v3z	2.98 (+4.1%)	12.52 (-0.8%)
dyall.v4z	2.91 (+1.7%)	12.58 (-0.4%)
CBS(M)	2.87 (+0.3%)	12.62 (-0.1%)
CBS(H)	2.86	12.63
CBS(L)	2.85 (-0.4%)	12.64 (+0.1%)
95% c.i.	0.02	0.02

TABLE V. Effect of the basis set cardinality (vnz , $n = 2, 3, 4$) on the W_d constants calculated using CCSD(T) with 17 correlated electrons and a virtual space cut-off of 30 a.u. for BaCH₃ and using FSCC with 29 electrons correlated and virtual space cut-off of 10 a.u. for YbCH₃. In the lower part of the table, results obtained using the different CBS extrapolation schemes and the respective uncertainty estimation are shown. Relative errors with respect to the CBS(H) limit are shown in parentheses.

we analyse the effect of the cardinality and the special features of the basis sets on the calculated W_d and W_s factors.

a. Complete basis set limit Table V presents the dependence of the calculated W_d constants on the cardinality of the basis set. Overall, W_d changes monotonically with increase of basis set cardinality. In BaCH₃ it decreases by 6.5% when going from 2z to 4z cardinality basis set, while in YbCH₃ it increases by 4.1%. We extrapolate our results to the complete basis set (CBS) limit, using the usual three-point Dunning–Feller $e^{-\alpha n}$ scheme ($n = 2, 3, 4$) [65, 66] for extrapolating the DHF energies and the two-point Helgaker et al. n^{-3} scheme ($n = 3, 4$) [67] for extrapolating the correlation energies. We also tested the Martin $(n + \frac{1}{2})^{-4}$ scheme [68] and the recent scheme of Lesiuk and Jeziorski (based on the application of the Riemann zeta function) [69] for extrapolating the correlation energies. The latter three extrapolation schemes (labeled H, M and L in Table V, respectively) give evenly spread and very similar CBS limits. We use the central Helgaker CBS limit for our final results and the respective 95% confidence interval (1.96σ) based on the spread of the three schemes as our extrapolation uncertainty estimate. The same methodology was used in our previous studies [70].

b. Core correlating and diffuse functions The results shown in Table VI showcase the effects of including outer- and inner-core correlating (cv3z, aev3z) and diffuse functions (aug-v3z) on the calculated W_d factors. The difference between the cv3z/ae3z basis set and the v3z basis set lies in the addition of tight functions with high angular momentum, namely, 2/5 f and 1/2 g functions for Ba atom and 1/1 d function for C. On the other hand, the difference between the aug-v3z and the v3z lies in the even-tempered addition of diffuse functions for each angular momentum in all the atoms. For BaCH₃ the two augmentation schemes cause changes that are similar in magnitude but opposite in sign, leading to a negligible net effect. The W_d in YbCH₃ shows a negligible depen-

Basis set	$W_d [10^{24} \frac{\text{hHz}}{\text{ecm}}]$	
	BaCH ₃	YbCH ₃
dyall.v3z	3.20	12.87
dyall.cv3z	3.26 (+1.71%)	12.88 (+0.05%)
dyall.ae3z	3.26 (+1.68%)	12.86 (-0.08%)
aug-dyall.v3z	3.15 (-1.74%)	12.87 (-0.02%)

TABLE VI. Effect of the basis set on the calculated W_d constants. The deviations relative to the dyall.v3z basis set are shown in parenthesis. CCSD(T) level of theory with 37 electrons correlated and virtual space cut-off of 60 a.u. for BaCH₃ and FSCC with 31 electrons correlated and virtual space cut-off of 20 a.u. for YbCH₃.

dence on both types of augmentation. In this case, the difference between the dyall.v3z and the dyall.cv3z basis sets is small since the two sets are identical for Yb and the only differences are in the number of the core-correlating functions on carbon. In the dyall.ae3z basis set for Yb, only one extra g function is added to the dyall.cv3z basis. Due to the small (and opposite) effects, we proceed with the non-augmented dyall.v3z basis sets for both molecules and we included the effect of the augmentation and including correlating functions in our uncertainty estimation.

C. Recommended values and uncertainty estimation

The extensive computational study carried out in the previous section allows us to determine the most suitable method for obtaining the recommended values of the W_d and the W_s constants of the two molecules.

For BaCH₃, we provide the final value of W_d calculated at the CCSD(T) level of theory using the dyall.v3z basis set, correlating all the electrons and including virtual orbitals up to 2000 a.u. giving the base value of $3.33 \times 10^{24} \frac{\text{hHz}}{\text{ecm}}$. To this, we add the CBS extrapolation correction of $-0.11 \times 10^{24} \frac{\text{hHz}}{\text{ecm}}$ evaluated correlating 17 electrons with a virtual space cut-off of 30 a.u. We estimated the uncertainty due to the finite basis set (cardinality, core correlating and diffuse basis functions) and due to the neglect of higher-order excitations based on the study in the previous sections. To determine the size of each source of error, we use the difference in W_d obtained with the final method and W_d obtained with a lower approximation (for a given computational parameter) as is schematically shown in Table VII. In addition, to estimate the uncertainty stemming from the molecular geometry optimisation, we calculated the W_d factor using the experimental geometry range (Ba–C bond distance = 2.557 – 2.570 Å [61]) and found that the maximum variation with respect to the value obtained using the optimised geometry is 1.08%. Finally, the Dirac–Coulomb Hamiltonian used in this work assumes an instantaneous (non-relativistic) electron–electron interaction. The Breit interaction is the first-order correction, and as it contains

Source of uncertainty		$\delta_i W_d [10^{24} \frac{h\text{Hz}}{\text{ecm}}] (\%)$		Scheme
		BaCH ₃	YbCH ₃	
Correlation	Virtual cut-off	0.017 (0.5%)	0.014 (0.1%)	2000 – 1000 a.u.
	Triples	0.029 (0.9%)	0.252 (1.8%)	CCSD(T) – CCSD
Basis set	CBS extrapolation	0.021 (0.7%)	0.020 (0.15%)	1.96 σ
	Diffuse functions	0.055 (1.7%)	0.003 (0.02%)	aug-v3z – v3z
	Core-correl. functions	0.055 (1.7%)	0.010 (0.07%)	ae3z – v3z
Geometry	Optimization	0.037 (1.2%)	0.160 (1.2%)	opt. – expt.
Relativity	Gaunt	0.057 (1.8%)	0.180 (1.3%)	Gaunt-DC – DC
Total uncertainty		0.111 (3.44%)	0.349 (2.53%)	$\sqrt{\sum_i \delta_i^2}$
Final recommended value		3.224 ± 0.111	13.799 ± 0.349	

TABLE VII. Summary of the most significant sources of uncertainty in W_d in BaCH₃ and YbCH₃ [$10^{24} \frac{h\text{Hz}}{\text{ecm}}$]. Values in parentheses represent the relative uncertainties with respect to the final results.

two-electron operators [71] it is not possible to separate this effect from the electron correlation effects. While aware of this limitation, we evaluate effect of the dominant Gaunt term of the Breit interaction [72] at the Dirac–Hartree–Fock (DHF) level of theory resulting in an decrease in W_d of 1.8%. We thus set an estimate of the uncertainty on our recommended values due to the missing Breit interaction and higher order effects to 1.8%. All the individual contributions to the uncertainty are summarised in Table VII and we estimate the total uncertainty (assuming the effects are independent) at 3.44%. The recommended value for BaCH₃ is thus $W_d = 3.224 \pm 0.111 \times 10^{24} \frac{h\text{Hz}}{\text{ecm}}$.

For YbCH₃, we provide the final value of W_d calculated at the FSCC level of theory, correlating all the electrons and including virtual orbitals up to 2000 a.u., as we did in BaCH₃. In YbCH₃ however, it was computationally unfeasible to correlate all the electrons when using the dyall.v3z basis. Nevertheless, since the effect of the correlation space is bigger than the effect of the size of the basis set, we employed the dyall.v2z basis set to obtain the base value of $13.25 \times 10^{24} \frac{h\text{Hz}}{\text{ecm}}$ and to this we added the CBS correction of $+0.56 \times 10^{24} \frac{h\text{Hz}}{\text{ecm}}$, evaluated correlating 29 electrons with a virtual space cut-off of 10 a.u. We used an analogous scheme to that employed for BaCH₃ to estimate the uncertainty of this result. However, since the experimental geometry is yet not known for YbCH₃, we use the same relative uncertainty due to the geometry optimisation as we derived for BaCH₃. This assumption is justified by the fact that we used the same methodology to optimise the geometry of the two molecules. Furthermore, to estimate the effect of the excitation rank, we include in our uncertainty estimation twice the relative uncertainty obtained for BaCH₃ to account for neglecting both the triples and the higher-order excitations. The recommended value for YbCH₃ is thus $W_d = 13.799 \pm 0.349 \times 10^{24} \frac{h\text{Hz}}{\text{ecm}}$.

Figure 4 presents the relative uncertainties for the different sources discussed above and calculated as described in Table VII. The highest contributions to the total uncertainty in BaCH₃ is due to the basis set incompleteness and the current limitation to describing the Breit interaction correctly. Notice that the addition

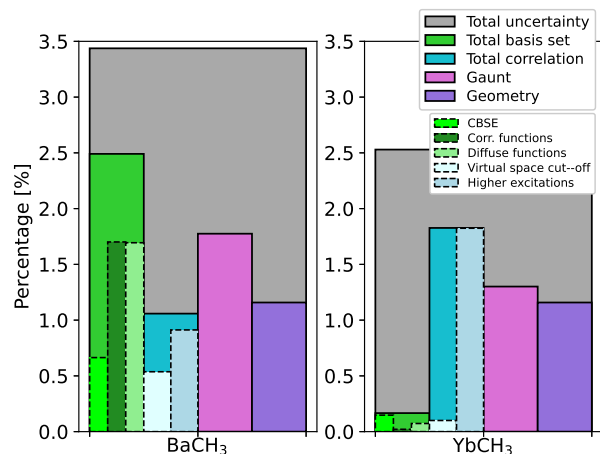


FIG. 4. Total and individual contributions to the uncertainty in percent relative to the recommended values (DC-CCSD(T), CBSE-corrected, and DC-FSCC, CBSE-corrected for BaCH₃ and YbCH₃, respectively).

of diffuse and extra correlating functions have an opposite effect, meaning that we over-estimate somewhat this source of uncertainty. In the case of YbCH₃, the employed basis set is highly converged. Consequently, the total uncertainty in W_d is smaller for YbCH₃ than for BaCH₃ with the leading source of uncertainty coming from the electron correlation description.

We have also performed calculations of the W_s parameters using the computational scheme employed for the recommended W_d values. The different computational parameters included in the uncertainty estimation in this work have effects of the same magnitude on the calculated W_d and W_s in BaF [37], with the Gaunt term being the only exception. In BaF, the Gaunt term, and therefore, the total uncertainty, is smaller in W_s than in W_d . Consequently, in this work we assume the relative uncertainty of the W_s values is on the same order of magnitude as the uncertainty found for the corresponding W_d factors. All the recommended values are summarised in Table VIII and compared to the earlier predictions for

Molecule	Method	W_d [$10^{24} \frac{h\text{Hz}}{\text{e.u.}}$]	W_s [kHz]
BaCH ₃	DC-CCSD(T)	3.22 ± 0.11	8.42 ± 0.29
BaOCH ₃	X2C-CCSD(T)	3.05 [73]	
BaOH	DC-CCSD(T)	3.10 ± 0.15 [38]	
	ZORA-cGHF	3.32 ± 0.33 [39]	8.79 ± 0.88 [39]
	ZORA-cGKS	2.98 ± 0.30 [39]	7.91 ± 0.79 [39]
BaF	DC-CCSD(T)	3.13 ± 0.12 [37]	8.29 ± 0.12 [37]
YbCH ₃	DC-FSCC(0,1)	13.80 ± 0.35	45.35 ± 1.15
YbOCH ₃	X2C-CCSD(T)	11.60 [73]	
YbOH	DC-FSCC(0,1)	11.30 ± 0.5 [38]	
	ZORA-cHFS	11.40 ± 1.14 [39]	41.2 ± 4.12 [39]
	ZORA-cGKS	8.54 ± 0.85 [39]	30.8 ± 3.08 [39]
	DC-CCSD	11.47 ± 0.68 [74]	
YbF	DC-FSCC	11.39 [37]	

TABLE VIII. Recommended W_d and W_s values of BaCH₃ and YbCH₃ and comparison to homologous molecules. A factor of 0.4835 was used to convert E_{eff} in GV/cm units to W_d in $10^{24} \frac{h\text{Hz}}{\text{e.u.}}$ units when necessary.

similar molecules.

D. Comparison and molecular bond analysis

The final calculated enhancement factors in BaCH₃ and YbCH₃ are of the same order of magnitude as in their corresponding isoelectronic linear molecules BaOH, BaF, YbOH, and YbF, and the non-linear polyatomic molecules BaOCH₃ and YbOCH₃, respectively. However, the enhancement factors in BaCH₃ and especially in YbCH₃ are larger than in the other molecules.

To investigate the origin of this difference, we calculated the W_d and W_s parameters for all the systems using the same approach and used the Quantum Theory of Atoms In Molecules (QTAIM) [75] and the Natural Bond Orbital (NBO) [76] analyses to study the relevant bonds. Table IX presents W_d and W_s obtained at the CCSD(T) and FSCC(0,1) level for the Ba- and Yb-containing molecules, respectively. To conserve computational effort, the dyall.v2z basis set was used and a cutoff was set at -2 to +10 a.u. for Ba- and -1 to +10 a.u. for Yb-containing systems. For the QTAIM and NBO analysis, we employ the SR-ZORA Hamiltonian with the PBE functional [77] and the QZ4P basis set in the Amsterdam density functional (ADF) package [78].

In the QTAIM analysis, intermolecular interactions can be characterized according to the topology of the electron density at the bond critical points (BCPs) denoted by \mathbf{r}_c . Specifically, the Espinoza and coworkers criteria [79] classify the bonding interactions according to the ratio of the potential $V(\mathbf{r}_c)$ and kinetic $G(\mathbf{r}_c)$ energy density at the BCPs, $|V(\mathbf{r}_c)|/G(\mathbf{r}_c)$. A ratios < 1 correspond to long-range, ionic or hydrogen bonds, values between 1 – 2 to intermediate bonds (with both ionic and covalent character) and ratios > 2 to covalent bonds. The ratio $|V(\mathbf{r}_c)|/G(\mathbf{r}_c)$ in Table IX suggests that the M–X (M = Ba, Yb; X = C, O, F) bonds can not be characterized as purely ionic bonds, and especially, the M–C

System	W_d [$10^{24} \frac{h\text{Hz}}{\text{e.u.}}$]	W_s [kHz]	$\frac{ V(\mathbf{r}_c) }{G(\mathbf{r}_c)}$	q_M
BaCH ₃	3.10	7.60	1.64	0.78
BaOCH ₃	2.79	6.88	1.20	0.88
BaOH	2.82	6.96	1.22	0.90
BaF	2.80	6.89	1.28	0.89
YbCH ₃	12.07	41.20	1.48	0.68
YbOCH ₃	9.89	33.98	1.12	0.82
YbOH	10.03	34.51	1.13	0.84
YbF	10.30	35.43	1.15	0.83
YbH	13.15	45.05	1.55	0.64

TABLE IX. Correlation between the W_d and W_s values of interest with bonding characteristics of the M–X bond (M = Ba, Yb; X = C, O, F). Espinoza criterion $\frac{|V(\mathbf{r}_c)|}{G(\mathbf{r}_c)}$ is a measure of covalent bond character. q_M represents the natural charge of the heavy element.

bonds have a significantly increased covalent character as compared to the M–O and M–F bonds. The natural charges based on natural atomic orbitals (NAOs) of the heavy atoms q_M support this observation. The M–C bonds are less polar compared to the M–O and M–F bonds. It means that in BaCH₃ and YbCH₃ molecules, the unpaired electron that experiences the P, T-odd interaction is more localized on the heavy atom, leading to a higher enhancement factor than for the other Ba-, Yb-containing molecules. We tested this conjecture by including YbH in our analysis, which follows the expected trend – the less electronegative hydrogen leads to more covalent bonding and an increase in the W_d and W_s values. A similar observation was made in previous works [80, 81].

IV. EXPERIMENTAL CONSIDERATIONS

BaCH₃ and YbCH₃ are both prime candidates for creation of intense beams via buffer gas cooling [82]. The rotational spectrum of the ground electronic state of BaCH₃ has been studied via millimeter/submillimeter absorption [83] and was created via the reaction of barium metal with Sn(CH₃)₄. Other alkaline-earth monomethyl molecules have been created via reaction of metals with other monomethyl species [84], including chloromethane (CH₃Cl) which could be used to react with ablated Yb or Ba metal in a cryogenic buffer gas cell. While YbCH₃ has not been studied spectroscopically, the chemical similarity of Yb with the alkaline-earth metals means that these production methods would likely work as well, as has been demonstrated with a number of other Yb-containing molecules [34, 85].

The P, T-violation measurement with these species would be performed in the $K = 1$ rotational state of the ground electronic and vibrational state, in which K -doubling splits the rotational states into doublets of opposite parity [27, 34, 86]. The state with $K = 1$ corresponds to the molecule rotating about its C_{3v} symmetry

axis with one quantum of angular momentum. Alkaline-earth metals bound to $-\text{CH}_3$ and $-\text{OCH}_3$ ligands have this state at roughly 160 GHz above the ground state [86–88], giving them lifetimes estimated to be minutes or longer. As this energy corresponds to ≈ 8 K, there will be appreciable population in a buffer gas source at a few Kelvin. The doubling in small, open-shell molecules with a metal-centered electron and a CH_3 group is dominated by anisotropic dipole-dipole interactions between the H nuclear spins and unpaired electron spin [34, 89]. For CaOCH_3 this has been measured to be around 300 kHz [89], but due to the closer distance between the metal and H_3 group in MCH_3 molecules this value is likely a few times larger, around 1 MHz. Note that the overall level structure, including the states which would be used for a spin precession measurement, are similar to other symmetric top molecules [86]. Also similar is that the EDM sensitivity would saturate to $\approx 50\%$ of the maximum values at the small fields required to mix the parity doublets [86, 90].

V. CONCLUSIONS

In this work, we report the enhancement factors W_d and W_s needed for the interpretation of possible eEDM measurements on the promising molecules BaCH_3 and YbCH_3 . We carried out a systematic study to devise a computationally feasible scheme that provides accurate predictions along with realistic uncertainties.

We showed that the scalar-relativistic level of theory in combination with the coupled cluster method and the ANO-RCC basis sets is a feasible and accurate approach for the optimisation of small polyatomic molecules. Correlating the valence and core-valence ($n-1$) and ($n-2$) electrons gives essentially the same results as correlating all electrons. The geometry obtained with this approach is in a very good agreement with the available experi-

mental reports (for BaCH_3).

The values of W_d and W_s calculated in this work for both BaCH_3 and YbCH_3 are slightly larger than in other Ba- and Yb-containing molecules. The relation between the increased covalent character of the heavy atom bond and the size of the W_d and W_s factors provides important insight for the search for promising candidates for precision experiments.

Accurate calculations of properties needed for interpretation of precision measurements in polyatomic molecules is a challenging task and it is necessary to methodically evaluate the effects of the most relevant computational parameters. In this work, we provide such analysis for the BaCH_3 and YbCH_3 molecules. We show that calculating the W_d and W_s values requires an accurate description of the electron correlation. Specifically, in the coupled cluster approach, the number of electrons included in the correlation description plays the most significant role. The size of the basis set has a comparatively smaller but non-negligible effect. The systematic evaluation of the effect of various computational parameters also allowed us to estimate the uncertainty in the values presented in this work.

ACKNOWLEDGEMENTS

This publication is part of the project *High Sector Fock space coupled cluster method: benchmark accuracy across the periodic table* (with project number VI.Vidi.192.088 of the research programme Vidi which is financed by the Dutch Research Council (NWO)). We thank the Center for Information Technology of the University of Groningen for their support and for providing access to the Peregrine high performance computing cluster. LFP acknowledges the support from the Slovak Research and Development Agency (APVV-20-0098, APVV-20-0127).

-
- [1] G. Bertone, *Particle dark matter: observations, models and searches* (Cambridge University Press, 2010).
 - [2] J. Solà Peracaula, Cosmological constant and vacuum energy: Old and new ideas, *Journal of Physics Conference Series* **453** (2013).
 - [3] M. Dine and A. Kusenko, Origin of the matter-antimatter asymmetry, *Reviews of Modern Physics* **76**, 1 (2003).
 - [4] J. Ginges and V. V. Flambaum, Violations of fundamental symmetries in atoms and tests of unification theories of elementary particles, *Physics Reports* **397**, 63 (2004).
 - [5] Y. Yamaguchi and N. Yamanaka, Large long-distance contributions to the electric dipole moments of charged leptons in the standard model, *Physical Review Letters* **125**, 241802 (2020).
 - [6] E. D. Commins, Electric dipole moments of leptons, in *Advances in Atomic, Molecular, and Optical Physics*, Vol. 40 (Elsevier, 1999) pp. 1–55.
 - [7] W. Bernreuther and M. Suzuki, The electric dipole moment of the electron, *Reviews of Modern Physics* **63**, 313 (1991).
 - [8] M. Pospelov and A. Ritz, CKM benchmarks for electron electric dipole moment experiments, *Physical Review D* **89**, 056006 (2014).
 - [9] M. Sachs and S. L. Schwebel, Implications of parity non-conservation and time reversal noninvariance in electromagnetic interactions: Part II. Atomic energy levels, *Annals of Physics* **8**, 475 (1959).
 - [10] E. Salpeter, Some atomic effects of an electronic electric dipole moment, *Physical Review* **112**, 1642 (1958).
 - [11] M. Bouchiat and C. Bouchiat, I. Parity violation induced by weak neutral currents in atomic physics, *Journal de Physique* **35**, 899 (1974).
 - [12] P. Sandars, The electric dipole moment of an atom, *Physics Letters* **14**, 194 (1965).

- [13] P. Sandars, The electric-dipole moments of an atom II. the contribution from an electric-dipole moment on the electron with particular reference to the hydrogen atom, *Journal of Physics B: Atomic and Molecular Physics* **1**, 511 (1968).
- [14] P. Sandars, Measurability of the proton electric dipole moment, *Physical Review Letters* **19**, 1396 (1967).
- [15] D. DeMille, Diatomic molecules, a window onto fundamental physics, *Physics Today* **68**, 34 (2015).
- [16] G. Harrison, P. Sandars, and S. Wright, Experimental limit on the proton electric dipole moment, *Physical Review Letters* **22**, 1263 (1969).
- [17] E. Hinds, C. Loving, and P. Sandars, Limits on P and T violating neutral current weak interactions, *Physics Letters B* **62**, 97 (1976).
- [18] E. A. Hinds and P. Sandars, Experiment to search for P- and T-violating interactions in the hyperfine structure of thallium fluoride, *Physical Review A* **21**, 480 (1980).
- [19] V. Andreev and N. Hutzler, Improved limit on the electric dipole moment of the electron, *Nature* **562**, 355 (2018).
- [20] D. M. Kara, I. Smallman, J. J. Hudson, B. E. Sauer, M. R. Tarbutt, and E. A. Hinds, Measurement of the electron's electric dipole moment using YbF molecules: methods and data analysis, *New Journal of Physics* **14**, 103051 (2012).
- [21] W. B. Cairncross, D. N. Gresh, M. Grau, K. C. Cossel, T. S. Roussy, Y. Ni, Y. Zhou, J. Ye, and E. A. Cornell, Precision measurement of the electron's electric dipole moment using trapped molecular ions, *Physical Review Letters* **119**, 153001 (2017).
- [22] R. F. Garcia Ruiz, R. Berger, J. Billowes, C. Binnersley, M. Bissell, A. Breier, A. Brinson, K. Chrysalidis, T. Collois, B. Cooper, *et al.*, Spectroscopy of short-lived radioactive molecules, *Nature* **581**, 396 (2020).
- [23] T. Isaev, S. Hoekstra, and R. Berger, Laser-cooled RaF as a promising candidate to measure molecular parity violation, *Physical Review A* **82**, 052521 (2010).
- [24] P. Aggarwal, H. L. Bethlem, A. Borschevsky, M. Denis, K. Esajas, P. A. Haase, Y. Hao, S. Hoekstra, K. Jungmann, T. B. Meijknecht, *et al.*, Measuring the electric dipole moment of the electron in BaF, *The European Physical Journal D* **72**, 1 (2018).
- [25] S. Bickman, P. Hamilton, Y. Jiang, and D. DeMille, Preparation and detection of states with simultaneous spin alignment and selectable molecular orientation in PbO, *Physical Review A* **80**, 023418 (2009).
- [26] J. J. Hudson, D. M. Kara, I. Smallman, B. E. Sauer, M. R. Tarbutt, and E. A. Hinds, Improved measurement of the shape of the electron, *Nature* **473**, 493 (2011).
- [27] I. Kozyryev and N. R. Hutzler, Precision measurement of time-reversal symmetry violation with laser-cooled polyatomic molecules, *Physical Review Letters* **119**, 133002 (2017).
- [28] N. R. Hutzler, Polyatomic molecules as quantum sensors for fundamental physics, *Quantum Science and Technology* **5**, 044011 (2020).
- [29] A. M. Ellis, Main group metal-ligand interactions in small molecules: new insights from laser spectroscopy, *International Reviews in Physical Chemistry* **20**, 551 (2001).
- [30] T. Isaev, A. Zaitsevskii, and E. Eliav, Laser-coolable polyatomic molecules with heavy nuclei, *Journal of Physics B: Atomic, Molecular and Optical Physics* **50**, 225101 (2017).
- [31] T. A. Isaev and R. Berger, Polyatomic candidates for cooling of molecules with lasers from simple theoretical concepts, *Physical Review Letters* **116**, 063006 (2016).
- [32] I. Kozyryev, L. Baum, K. Matsuda, and J. M. Doyle, Proposal for laser cooling of complex polyatomic molecules, *ChemPhysChem* **17**, 3641 (2016).
- [33] D. Mitra, N. B. Vilas, C. Hallas, L. Anderegg, B. L. Augenbraun, L. Baum, C. Miller, S. Raval, and J. M. Doyle, Direct laser cooling of a symmetric top molecule, *Science* **369**, 1366 (2020).
- [34] B. L. Augenbraun, Z. D. Lasner, A. Frenett, H. Sawaoka, A. T. Le, J. M. Doyle, and T. C. Steimle, Observation and laser spectroscopy of ytterbium monomethoxide, YbOCH₃, *Physical Review A* **103**, 022814 (2021).
- [35] M. G. Kozlov and L. N. Labzowsky, Parity violation effects in diatomics, *Journal of Physics B: Atomic, Molecular and Optical Physics* **28**, 1933 (1995).
- [36] M. Kozlov and V. Ezhov, Enhancement of the electric dipole moment of the electron in the YbF molecule, *Physical Review A* **49**, 4502 (1994).
- [37] P. A. B. Haase, D. J. Doeglas, A. Boeschoten, E. Eliav, M. Iliáš, P. Aggarwal, H. L. Bethlem, A. Borschevsky, K. Esajas, Y. Hao, S. Hoekstra, V. R. Marshall, T. B. Meijknecht, M. C. Mooij, K. Steinebach, R. G. E. Timmermans, A. P. Touwen, W. Ubachs, L. Willmann, and Y. Y. and, Systematic study and uncertainty evaluation of P,T-odd molecular enhancement factors in BaF, *The Journal of Chemical Physics* **155**, 034309 (2021).
- [38] M. Denis, P. A. Haase, R. G. Timmermans, E. Eliav, N. R. Hutzler, and A. Borschevsky, Enhancement factor for the electric dipole moment of the electron in the BaOH and YbOH molecules, *Physical Review A* **99**, 042512 (2019).
- [39] K. Gaul and R. Berger, Ab initio study of parity and time-reversal violation in laser-coolable triatomic molecules, *Physical Review A* **101**, 012508 (2020).
- [40] A.-M. Mårtensson-Pendrill and P. Öster, Calculations of atomic electric dipole moments, *Physica Scripta* **36**, 444 (1987).
- [41] H. D. Cohen and C. Roothaan, Electric dipole polarizability of atoms by the Hartree—Fock method. I. Theory for closed-shell systems, *The Journal of Chemical Physics* **43**, S34 (1965).
- [42] L. Visscher, T. Enevoldsen, T. Saue, and J. Oddershede, Molecular relativistic calculations of the electric field gradients at the nuclei in the hydrogen halides, *The Journal of Chemical Physics* **109**, 9677 (1998).
- [43] Y. Hao, M. Iliáš, E. Eliav, P. Schwerdtfeger, V. V. Flambaum, and A. Borschevsky, Nuclear anapole moment interaction in BaF from relativistic coupled-cluster theory, *Physical Review A* **98**, 032510 (2018).
- [44] Y. Hao, P. Navrátil, E. B. Norrgard, M. Iliáš, E. Eliav, R. G. E. Timmermans, V. V. Flambaum, and A. Borschevsky, Nuclear spin-dependent parity-violating effects in light polyatomic molecules, *Phys. Rev. A* **102**, 052828 (2020).
- [45] P. A. B. Haase, E. Eliav, M. Iliáš, and A. Borschevsky, Hyperfine structure constants on the relativistic coupled cluster level with associated uncertainties, *The Journal of Physical Chemistry A* **124**, 3157 (2020).
- [46] M. Denis, P. A. Haase, M. C. Mooij, Y. Chamorro, P. Aggarwal, H. L. Bethlem, A. Boeschoten, A. Borschevsky, K. Esajas, Y. Hao, *et al.*, Benchmarking of the Fock

- space coupled cluster method and uncertainty estimation: Magnetic hyperfine interaction in the excited state of BaF, *Physical Review A* **105**, 052811 (2022).
- [47] T. Chupp, P. Fierlinger, M. Ramsey-Musolf, and J. Singh, Electric dipole moments of atoms, molecules, nuclei, and particles, *Reviews of Modern Physics* **91**, 015001 (2019).
- [48] DIRAC, a relativistic ab initio electronic structure program, Release DIRAC19 (2019), written by A. S. P. Gomes, T. Saue, L. Visscher, H. J. Aa. Jensen, and R. Bast, with contributions from I. A. Aucar, V. Bakken, K. G. Dyall, S. Dubillard, U. Ekström, E. Eliav, T. Enevoldsen, E. Faßhauer, T. Fleig, O. Fossgaard, L. Halbert, E. D. Hedegård, B. Heimlich–Paris, T. Helgaker, J. Henriksson, M. Iliáš, Ch. R. Jacob, S. Knecht, S. Komorovský, O. Kullie, J. K. Lærdahl, C. V. Larsen, Y. S. Lee, H. S. Nataraj, M. K. Nayak, P. Norman, G. Olejniczak, J. Olsen, J. M. H. Olsen, Y. C. Park, J. K. Pedersen, M. Pernpointner, R. di Remigio, K. Ruud, P. Salek, B. Schimmelpfennig, B. Senjean, A. Shee, J. Sikkema, A. J. Thorvaldsen, J. Thyssen, J. van Stralen, M. L. Vidal, S. Villaume, O. Visser, T. Winther, and S. Yamamoto (available at <https://doi.org/10.5281/zenodo.3572669>, see also <http://www.diracprogram.org>).
- [49] T. Saue, R. Bast, A. S. P. Gomes, H. J. A. Jensen, L. Visscher, I. A. Aucar, R. Di Remigio, K. G. Dyall, E. Eliav, E. Fasshauer, *et al.*, The DIRAC code for relativistic molecular calculations, *The Journal of Chemical Physics* **152**, 204104 (2020).
- [50] J. F. Stanton, J. Gauss, L. Cheng, M. E. Harding, D. A. Matthews, and P. G. Szalay, CFOUR, Coupled-Cluster techniques for Computational Chemistry, a quantum-chemical program package, With contributions from A.A. Auer, R.J. Bartlett, U. Benedikt, C. Berger, D.E. Bernholdt, S. Blaschke, Y. J. Bomble, S. Burger, O. Christiansen, D. Datta, F. Engel, R. Faber, J. Greiner, M. Heckert, O. Heun, M. Hilgenberg, C. Huber, T.-C. Jagau, D. Jonsson, J. Jusélius, T. Kirsch, K. Klein, G.M. KopperW.J. Lauderdale, F. Lipparini, T. Metzroth, L.A. Mück, D.P. O’Neill, T. Nottoli, D.R. Price, E. Prochnow, C. Puzzarini, K. Ruud, F. Schiffmann, W. Schwalbach, C. Simmons, S. Stopkowicz, A. Tajti, J. Vázquez, F. Wang, J.D. Watts and the integral packages MOLECULE (J. Almlöf and P.R. Taylor), PROPS (P.R. Taylor), ABACUS (T. Helgaker, H.J. Aa. Jensen, P. Jørgensen, and J. Olsen), and ECP routines by A. V. Mitin and C. van Wüllen. For the current version, see <http://www.cfour.de>.
- [51] D. A. Matthews, L. Cheng, M. E. Harding, F. Lipparini, S. Stopkowicz, T.-C. Jagau, P. G. Szalay, J. Gauss, and J. F. Stanton, Coupled-cluster techniques for computational chemistry: The program package, *The Journal of Chemical Physics* **152**, 214108 (2020).
- [52] L. Visscher, T. J. Lee, and K. G. Dyall, Formulation and implementation of a relativistic unrestricted coupled-cluster method including noniterative connected triples, *The Journal of Chemical Physics* **105**, 8769 (1996).
- [53] L. Visscher, E. Eliav, and U. Kaldor, Formulation and implementation of the relativistic fock-space coupled cluster method for molecules, *The Journal of Chemical Physics* **115**, 9720 (2001).
- [54] K. G. Dyall, Relativistic double-zeta, triple-zeta, and quadruple-zeta basis sets for the 4s, 5s, 6s, and 7s elements, *The Journal of Physical Chemistry A* **113**, 12638 (2009).
- [55] A. S. Gomes, K. G. Dyall, and L. Visscher, Relativistic double-zeta, triple-zeta, and quadruple-zeta basis sets for the lanthanides La–Lu, *Theoretical Chemistry Accounts* **127**, 369 (2010).
- [56] K. G. Dyall, Relativistic double-zeta, triple-zeta, and quadruple-zeta basis sets for the light elements H–Ar, *Theoretical Chemistry Accounts* **135**, 128 (2016).
- [57] B. O. Roos, V. Veryazov, and P.-O. Widmark, Relativistic atomic natural orbital type basis sets for the alkaline and alkaline-earth atoms applied to the ground-state potentials for the corresponding dimers, *Theoretical Chemistry Accounts* **111**, 345 (2004).
- [58] B. O. Roos, R. Lindh, P.-Å. Malmqvist, V. Veryazov, and P.-O. Widmark, Main group atoms and dimers studied with a new relativistic ANO basis set, *The Journal of Physical Chemistry A* **108**, 2851 (2004).
- [59] B. O. Roos, R. Lindh, P.-Å. Malmqvist, V. Veryazov, P.-O. Widmark, and A. C. Borin, New relativistic atomic natural orbital basis sets for lanthanide atoms with applications to the ce diatom and LuF₃, *The Journal of Physical Chemistry A* **112**, 11431 (2008).
- [60] P.-O. Widmark, P.-Å. Malmqvist, and B. O. Roos, Density matrix averaged atomic natural orbital (ANO) basis sets for correlated molecular wave functions, *Theoretica chimica acta* **77**, 291 (1990).
- [61] J. Xin, J. Robinson, A. Apponi, and L. M. Ziurys, High resolution spectroscopy of BaCH₃ (\tilde{X}^2A_1): Fine and hyperfine structure analysis, *The Journal of Chemical Physics* **108**, 2703 (1998).
- [62] L. Schiff, Measurability of nuclear electric dipole moments, *Physical Review* **132**, 2194 (1963).
- [63] L. Pašteka, R. Mawhorter, and P. Schwerdtfeger, Relativistic coupled-cluster calculations of the ¹⁷³Yb nuclear quadrupole coupling constant for the YbF molecule, *Molecular Physics* **114**, 1110 (2016).
- [64] T. J. Lee and P. R. Taylor, A diagnostic for determining the quality of single-reference electron correlation methods, *International Journal of Quantum Chemistry* **36**, 199 (1989).
- [65] T. H. Dunning Jr, Gaussian basis sets for use in correlated molecular calculations. I. The atoms boron through neon and hydrogen, *The Journal of Chemical Physics* **90**, 1007 (1989).
- [66] D. Feller, Application of systematic sequences of wave functions to the water dimer, *The Journal of Chemical Physics* **96**, 6104 (1992).
- [67] T. Helgaker, W. Klopper, H. Koch, and J. Noga, Basis-set convergence of correlated calculations on water, *The Journal of Chemical Physics* **106**, 9639 (1997).
- [68] J. M. Martin, Ab initio total atomization energies of small molecules—towards the basis set limit, *Chemical Physics letters* **259**, 669 (1996).
- [69] M. Lesiuk and B. Jeziorski, Complete basis set extrapolation of electronic correlation energies using the Riemann zeta function, *Journal of Chemical Theory and Computation* **15**, 5398 (2019).
- [70] Y. Guo, L. F. Pašteka, E. Eliav, and A. Borschevsky, Ionization potentials and electron affinity of oganesson with relativistic coupled cluster method, in *Advances in Quantum Chemistry*, Vol. 83 (Elsevier, 2021) pp. 107–123.

- [71] E. Lindroth, B. Lynn, and P. Sandars, Order α^2 theory of the atomic electric dipole moment due to an electric dipole moment on the electron, *Journal of Physics B: Atomic, Molecular and Optical Physics* **22**, 559 (1989).
- [72] J. A. Gaunt, IV. The triplets of helium, *Philosophical Transactions of the Royal Society of London. Series A, Containing Papers of a Mathematical or Physical Character* **228**, 151 (1929).
- [73] C. Zhang, X. Zheng, and L. Cheng, Calculations of time-reversal-symmetry-violation sensitivity parameters based on analytic relativistic coupled-cluster gradient theory, *Physical Review A* **104**, 012814 (2021).
- [74] V. Prasanna, N. Shitara, A. Sakurai, M. Abe, and B. Das, Enhanced sensitivity of the electron electric dipole moment from YbOH: The role of theory, *Physical Review A* **99**, 062502 (2019).
- [75] R. F. Bader and T. Nguyen-Dang, Quantum theory of atoms in molecules—dalton revisited, in *Advances in Quantum Chemistry*, Vol. 14 (Elsevier, 1981) pp. 63–124.
- [76] E. D. Glendening, C. R. Landis, and F. Weinhold, Nbo 6.0: Natural bond orbital analysis program, *Journal of computational chemistry* **34**, 1429 (2013).
- [77] J. P. Perdew, K. Burke, and M. Ernzerhof, Generalized gradient approximation made simple, *Phys. Rev. Lett.* **77**, 3865 (1996).
- [78] G. t. Te Velde, F. M. Bickelhaupt, E. J. Baerends, C. Fonseca Guerra, S. J. van Gisbergen, J. G. Snijders, and T. Ziegler, Chemistry with *adf*, *Journal of Computational Chemistry* **22**, 931 (2001).
- [79] E. Espinosa, I. Alkorta, J. Elguero, and E. Molins, From weak to strong interactions: A comprehensive analysis of the topological and energetic properties of the electron density distribution involving X–H \cdots F–Y systems, *The Journal of chemical physics* **117**, 5529 (2002).
- [80] A. Sunaga, M. Abe, M. Hada, and B. Das, Analysis of large effective electric fields of weakly polar molecules for electron electric-dipole-moment searches, *Physical Review A* **95**, 012502 (2017).
- [81] E. R. Meyer, J. L. Bohn, and M. P. Deskevich, Candidate molecular ions for an electron electric dipole moment experiment, *Physical Review A* **73**, 062108 (2006).
- [82] N. R. Hutzler, H.-I. Lu, and J. M. Doyle, The buffer gas beam: an intense, cold, and slow source for atoms and molecules., *Chemical Reviews* **112**, 4803 (2012).
- [83] J. Xin, J. S. Robinson, A. J. Apponi, and L. M. Ziurys, High resolution spectroscopy of BaCH₃(\tilde{X}^2A_1): Fine and hyperfine structure analysis, *The Journal of Chemical Physics* **108**, 2703 (1998).
- [84] C. R. Brazier and P. F. Bernath, Observation of gas phase organometallic free radicals: Monomethyl derivatives of calcium and strontium, *The Journal of Chemical Physics* **86**, 5918 (1987).
- [85] A. Jadbabaie, N. H. Pilgram, J. Kłos, S. Kotochigova, and N. R. Hutzler, Enhanced molecular yield from a cryogenic buffer gas beam source via excited state chemistry, *New Journal of Physics* **22**, 022002 (2020).
- [86] P. Yu and N. R. Hutzler, Probing fundamental symmetries of deformed nuclei in symmetric top molecules, *Physical Review Letters* **126**, 10.1103/physrevlett.126.023003 (2021).
- [87] K. ichi C. Namiki and T. C. Steimle, Pure rotational spectrum of CaCH₃(\tilde{X}^2A_1) using the pump/probe microwave-optical double resonance (PPMODR) technique, *The Journal of Chemical Physics* **110**, 11309 (1999).
- [88] P. M. Sheridan, M. J. Dick, J.-G. Wang, and P. F. Bernath, High-resolution spectroscopic investigation of the $\tilde{B}^2A_1 - \tilde{X}^2A_1$ transitions of CaCH₃ and SrCH₃, *The Journal of Physical Chemistry A* **109**, 10547 (2005).
- [89] K. ichi C. Namiki, J. S. Robinson, and T. C. Steimle, A spectroscopic study of caoch₃ using the pump/probe microwave and the molecular beam/optical stark techniques, *The Journal of Chemical Physics* **109**, 5283 (1998).
- [90] A. Petrov and A. Zakharova, Sensitivity of the yboh molecule to p t-odd effects in an external electric field, *Physical Review A* **105**, L050801 (2022).
- [91] M. Iliaš and T. Saue, An infinite-order two-component relativistic hamiltonian by a simple one-step transformation, *The Journal of Chemical Physics* **126**, 064102 (2007).
- [92] T. Saue, Relativistic hamiltonians for chemistry: A primer, *ChemPhysChem* **12**, 3077 (2011).
- [93] W. Zou, M. Filatov, and D. Cremer, Development and application of the analytical energy gradient for the normalized elimination of the small component method, *The Journal of Chemical Physics* **134**, 244117 (2011).

VI. APPENDIX

A. Geometry optimization

1. Treatment of relativity

Relativistic effects play an indispensable role in the correct description of molecules containing heavy elements. However, inclusion of just the scalar relativistic effects is often sufficient to describe properties that are not very sensitive to the spin components, such as molecular geometry. This of course holds only for systems where the spin-orbit effects are not expected to be significant for the valence electrons, such as closed shell molecules or systems with valence s/σ orbitals. We test this assumption by comparing the geometries of BaCH₃ obtained within the 4-component (4c) and the exact 2-component (X2C) [91, 92] approaches and using the spin-free exact two-component one-electron variant formalism (SR) [93]. The first two methods were employed within the DIRAC19 program, while the SR calculations were performed using the CFOUR package. In Table X, it is observed that the X2C approach predicts the same results as the Dirac-Coulomb 4c Hamiltonian. Similarly the SR calculations differ in only 0.5% to the 4c and X2C results. Consequently, the use of the computationally less expensive SR level of theory is justified in the geometry optimisation of BaCH₃ and YbCH₃ and similar molecules.

Rel.	Basis set	Ba-C [Å]	C-H [Å]	BaCH [°]
4c	dyall.v2z	2.670	1.110	113.6
X2C	dyall.v2z	2.670	1.110	113.6
SR	dyall.v2z	2.657	1.108	113.2
SR	ANO.VDZ	2.613	1.107	112.7
X2C	dyall.v3z	2.605	1.100	112.8
SR	ANO.VTZ	2.585	1.098	112.6

TABLE X. Effect of the different levels of treatment of relativity on the optimised geometry of BaCH₃ at the CCSD level of theory. In all cases, 37 electrons were correlated.

2. Contracted vs. uncontracted basis set

In electronic structure calculations, contracted basis functions constructed from Gaussians perform for many properties with similar accuracy but with dramatically reduced computational costs compared to uncontracted basis sets. In the geometry optimisation of BaCH₃ and YbCH₃ (Table X), we observe that the scalar-relativistic approximation introduces a smaller error compared to the effect of the basis set contraction. The difference between the results obtained using contracted ANO-RCC.VDZ and uncontracted dyall.v2z basis sets at the SR level is 1.7%. However, this difference is reduced to 0.8% when comparing the larger SR-ANO-RCC.VTZ and X2C-dyall.v3z methods. This is expected, since with the increasing cardinality, the basis sets become more saturated and thus the negative effect of contraction should decrease. We thus proceed with the computationally less expensive ANO-RCC basis sets. Based on the results in Table X, when selecting basis sets for geometry optimisations considering their cost-benefit values, it is advisable to choose a higher cardinality contracted basis set over an uncontracted but lower cardinality one.

3. Electron correlation

Table XI contains comparison between the results obtained within the CCSD and the CCSD(T) approaches. The calculations were carried out within the single-reference framework and 37 electrons were correlated. We observe that inclusion of perturbative triple excitations has a minor effect on the obtained geometry (0.2% and 0.3% at the DZ and TZ basis set cardinality, respectively) and thus conclude that optimisation on the CCSD level is of sufficient quality when computational resources are of importance.

Furthermore, as expected, we find that the molecular geometry is a property mainly dependent on the valence

region of the molecule. Table XI shows that calculations correlating 37 electrons reproduce the all-electron results.

Method	N	Ba-C [Å]	C-H [Å]	BaCH [°]
ANO-RCC.VDZ				
CCSD	37	2.613	1.107	113
CCSD(T)	37	2.609	1.109	113
ANO-RCC.VTZ				
CCSD	37	2.586	1.098	113
CCSD(T)	37	2.579	1.099	113
CCSD(T)	65	2.578	1.099	113
CCSD(T)	27	2.591	1.102	113
CCSD(T)	17	2.606	1.102	113

TABLE XI. Effect of the perturbative triple excitations on the optimised geometry of BaCH₃, at the SR level of theory. N represents the number of correlated electrons.

B. Numerical stability of the FFPT

According to equations (6) and (7), the W_d and W_s factors can be calculated as the first derivatives of the energy with respect to the corresponding perturbation. To calculate the derivative using numerical differentiation, it is necessary to determine the field strength at which the total energy depends linearly on the perturbation. Figure 5 shows the dependence of the total energy in BaCH₃ on the λ_{d_e} perturbation. Linear behavior is found at smaller fields of the order $\lambda_{d_e} = 10^{-8}$ a.u. Similarly, for the W_s factor, the total energy is found to be linear at $\lambda_{k_s} = 10^{-7}$ a.u. In YbCH₃, $\lambda_{d_e} = \lambda_{k_s} = 10^{-6}$ a.u. correspond to the linear regime. To support these small fields, the convergence criterion of the coupled cluster energy as well as the Hartree-Fock energy was fixed at 10^{-11} a.u.

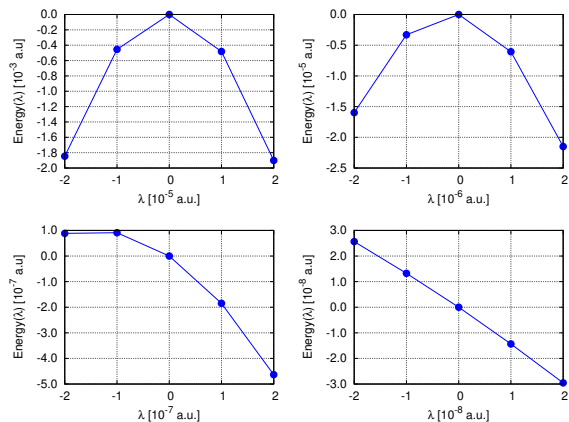


FIG. 5. Energy dependency with the field strength in BaCH₃. 4c-CCSD and dyall.v2z basis set were used.